

Article

Study of Probiotic Bacteria Encapsulation for Potential Application in Enrichment of Fermented Beverage

Galiya Madybekova ¹, Elmira Turkeyeva ², Botagoz Mutaliyeva ^{2,*} , Dinara Osmanova ², Saule Aidarova ³, Reinhard Miller ⁴ , Altynai Sharipova ⁵ and Assem Issayeva ³

- ¹ Chemistry Department, O. Zhanibekov South-Kazakhstan Pedagogical University, Shymkent 160012, Kazakhstan; galiya56@list.ru
- ² Biotechnology Department, M. Auezov South-Kazakhstan University, Shymkent 160012, Kazakhstan; turkeeva_1980@mail.ru (E.T.); dinaraosmanova0113@gmail.com (D.O.)
- ³ “One Belt, On Road” Petroleum Engineering Institute, Kazakh-British Technical University, Almaty 050000, Kazakhstan; ainano9999@gmail.com (S.A.); isa-aseem@mail.ru (A.I.)
- ⁴ Soft Matter Biophysics, Technische Universität Darmstadt, 64289 Darmstadt, Germany; reinhard.miller@pkm.tu-darmstadt.de
- ⁵ Mining and Metallurgical Institute, Satbayev University, Almaty 050013, Kazakhstan; a_sharipova85@mail.ru
- * Correspondence: botagoz.mutaliyeva@auuezov.edu.kz; Tel.: +7-7011298090

Abstract: The current work is devoted to the development of probiotic microencapsulation systems with the co-encapsulation of a plant extract, which can increase the survival of beneficial bacteria and are suitable for potential applications in the enrichment of fermented beverages based on acid whey. The encapsulation process exhibited a high level of effectiveness, achieving 83.0% for *Bifidobacterium* (BB), 89.2% for Stevia leaf extract (SE), and 91.3% for their combination (BB + SE). The FTIR analysis verified substantial interactions between the encapsulated agents and the polymer matrix, which enhanced the stability of the microcapsules. The BB + SE microcapsules exhibited reduced swelling and moisture content, indicating a denser structure compared to separately encapsulated BB and SE. Comparison of release kinetics of BB, SE and BB + SE loaded microcapsules showed that the combination of active agents has a quicker initial release, reaching 60% release within the first 2 h, and this value increased to 70% after 4 h. The release kinetics studies demonstrated a controlled release of active substances over 24 h. A morphology analysis shows that the surfaces of the dry microcapsules containing BB, SE, and their combination BB + SE have a porous structure. For encapsulated agents, the size of the capsules produced with BB and SE are smaller than those produced with two components (BB + SE), the sizes of which are between 760 μm and 1.1 mm. Modeling of the behavior of microcapsules in a simulated gastrointestinal tract provides information on swelling and active agents release rates as a function of pH in real biological environments. Thus, the new formulations of microcapsules with microorganisms and plant extracts have great potential for the development of fermented whey-based beverages.

Keywords: acid whey; encapsulation; *Bifidobacterium bifidum*; *Stevia rebaudiana Bertoni*; active agents; release; morphology; size; swelling degree; encapsulation efficiency



Citation: Madybekova, G.; Turkeyeva, E.; Mutaliyeva, B.; Osmanova, D.; Aidarova, S.; Miller, R.; Sharipova, A.; Issayeva, A. Study of Probiotic Bacteria Encapsulation for Potential Application in Enrichment of Fermented Beverage. *Colloids Interfaces* **2024**, *8*, 51. <https://doi.org/10.3390/colloids8050051>

Academic Editor: Francesco Lopez

Received: 26 June 2024

Revised: 1 September 2024

Accepted: 2 September 2024

Published: 6 September 2024



Copyright: © 2024 by the authors. Licensee MDPI, Basel, Switzerland. This article is an open access article distributed under the terms and conditions of the Creative Commons Attribution (CC BY) license (<https://creativecommons.org/licenses/by/4.0/>).

1. Introduction

Whey is a byproduct of cheese production; it is rich in carbon and nitrogen and contains high concentrations of lactose, proteins, and minerals [1,2]. There are two types of whey: sweet whey, which remains after enzymatic milk coagulation, and acid whey, which remains after milk coagulation via acidification [3]. As described in [4], acid whey is limited in its application because of its low pH and lactose content, and it mostly remains unused, creating environmental problems in terms of polluting water, soil, etc. [5].

There are many challenges to utilizing acid whey, but, at the same time, it is very attractive due to its richness in micro- and macro-elements. For example, the calcium

content of acid whey is two times higher than that of sweet whey, and this increases the value of acidic whey for obtaining fermented beverages and other products.

With added probiotic bacteria, acid whey can be used to obtain fermented beverages with properties beneficial to health [6]. Many of the health benefits of probiotics are associated with their survivability and stability in carrier food and under gastrointestinal conditions.

Fermented beverages are beneficial to the host only when the probiotics are administered in adequate amounts [7]. The fundamental properties of probiotics are resistance to stomach acid and tolerance to bile salts, as these properties allow them to survive acidic stomach conditions and the presence of bile salts in the small intestine during passage through the GIT [8].

However, several harsh conditions threaten their survival rate during processing, storage, and transit through the gastrointestinal tract (GIT), as well as possible interactions with beverage constituents during the incorporation of probiotics into beverages [9].

As noted by the authors of [10], most probiotics cannot survive in large quantities due to the low pH of gastric juice, which limits their effectiveness in most functional foods. Scientists have studied and compared free and capsulated probiotic microorganisms and concluded that probiotics protected by capsules showed the best results for bioavailability and survival in a gastrointestinal simulation [11].

Traditional techniques for maintaining the survival of probiotics during processing and storage are the selection of resistant strains, the inclusion of protective compounds, oxygen control, adaptation to stress, two-stage fermentation, and the addition of prebiotic substances [12]. Other authors [13] had the idea that enriching the alginate matrix used for probiotic encapsulation with whey as a substrate can have an impact on the antioxidant capacity and stability of whey-based beverages. They used whey as a substrate for fermentation to create a functional beverage and to solve environmental problems such as water contamination. This work emphasizes that encapsulation can not only solve the problem of preserving the viability of probiotics but can also increase the antioxidant properties of functional beverages. Zanjani et al. [14] stated that microencapsulation is one of the most modern methods for aiding probiotic survival and that the development of corresponding delivery systems can allow for the preservation and prolongation of probiotic activity [15]. Yao et al. [15] presented a new strategy for the microencapsulation of probiotics, and they highlighted the key mechanisms of their stress-resistant properties. They reviewed the latest *in vitro* and *in vivo* models to evaluate the effectiveness of probiotic delivery systems, and they emphasized the importance of having suitable models that can protect probiotics from aggressive environments.

Thus, probiotic microorganisms are encapsulated to ensure their survival during processing and storage and to protect them from the harmful effects of gastric pH and bile salts in order to ensure maximum bioavailability in the host [16]. Not only is encapsulation a solution to the problem of preserving the viability of probiotics, but it can also increase the antioxidant properties of functional beverages. Furthermore, using prebiotics in combination can selectively promote the growth and activity of beneficial bacteria and significantly maintain the survival of probiotics during processing and storage [12].

Currently, the development of delivery systems (in particular, microencapsulation systems) for various probiotic drugs, with the aim of overcoming the above-mentioned challenges [17], is the topic of many studies.

The composition of encapsulating material is the main determinant of microcapsule functional properties [18], and processing variables such as the concentration, characteristics of the core and coating materials, and stability, as well as the functionality and release kinetics of the desired product, can serve as criteria for the selection of matrix polymers to achieve efficient and effective encapsulation [19].

The effect of various encapsulating materials on the stability of probiotic bacteria was studied in [17], and it was found that microcapsules with alginate, xanthan gum, and carrageenan gum significantly improved the vitality of probiotic bacteria when exposed to acidic conditions and bile acid salts.

Alginate is commonly used to encapsulate probiotics because it is a promising system for their delivery [20]. In comparison with biomolecules such as polysaccharides (chitosan, xanthan, dextrin, and carrageenan) and milk proteins, sodium alginate is used more often because of its low costs and easy accessibility; it is also biocompatible and nontoxic [20,21].

Chitosan is the second most abundant biopolymer in the world, following cellulose. It is a versatile biopolymer with unique properties, and it is nontoxic, biodegradable, and biocompatible [22].

Zanjani et al. [14] found that alginate microcapsules can be coated by oppositely charged biopolymers, such as chitosan, leading to a strong interaction between the carboxylic groups of alginate and the amine groups of chitosan, resulting in enhanced stability of the microcapsules.

Moreover, the choice of appropriate methods is important because probiotics are highly sensitive and can lose their viability during encapsulation under different conditions. Mild techniques like spray-drying, extrusion, emulsification, and lyophilization are suitable with materials such as polysaccharides, proteins, and their complexes [23].

The two most commonly employed methods for obtaining microcapsules are emulsion and non-emulsion techniques. The encapsulation of probiotic drugs using emulsions provides stability by utilizing polyelectrolyte complexes that can be sustained in a wide range of external conditions (pH, ionic strength, and temperature). However, at the same time, this method is more complicated and consists of many formulation steps: an oil-in-water emulsion is produced and then mixed with the encapsulated materials. For water-soluble substances, the process involves creating a primary emulsion followed by the formation of a secondary emulsion, where the active ingredients are covered by envelope materials.

The second technique is simpler and based on direct microencapsulation with biopolymers (chitosan and alginate) without an emulsification step [24,25]. This is more suitable for microorganisms because of the absence of organic solvents.

Recently, not only probiotics but also various additives with prebiotic properties, such as Stevia, have been used to develop functional beverages. Several publications have described various reasons for using prebiotics. Combinations of several polysaccharides (alginate, κ -carrageenan, locust bean gum, gellan gum, and xanthan gum) with prebiotics (resistant starch, lactulose, and lactosucrose) and their effects on the encapsulation of the *Lactobacillus casei* 01 strain were studied, and higher survivability and protection [26] were observed. The addition of natural prebiotics (potato starch, *Plantago psyllium*, or inulin) to systems was found to improve the viability of *Lactobacillus casei* Shirota and two species of *Lactobacillus plantarum* (Lp17 and Lp33) [27]. Functional products such as stirred yogurt fortified with the prebiotic xylooligosaccharide and probiotic and synbiotic microcapsules were described by Ismail et al. [28]. The effect of inulin on the metabolic characteristics of probiotic yeast was studied, and it was found to affect the functionality of ice cream, increasing survivability and allowing for a long storage time [29]. Thus, prebiotics increase the metabolism of probiotics and maintain their survival during processing and storage [30].

The encapsulation of probiotics with Stevia extract as a prebiotic can solve problems related not only to the vitality and stability of beneficial microorganisms but also substitute carbohydrates with high glycemic indices, which improve their effects on human health [31].

Thus, the aim of the present work is to study the development of delivery systems for probiotics with a co-encapsulated plant extract that can increase survivability, prolong the positive nutrition effects on the human intestinal microflora, and have potential application for the enrichment of fermented beverages based on acid whey.

The preferred probiotic microorganisms are members of the genus *Bifidobacterium*, which are used in many foods and often added to dairy products.

There are many scientific reports on the description and health-promoting properties of *Bifidobacterium* [32]. It is known that *Bifidobacterium* (belonging to the phylum Actinobacteria) is the most commonly used and safe human probiotic, as certified by the

Food and Drug Administration (FDA) with the acronym GRAS (Generally Recognized As Safe) and by the European Food Safety Authority (EFSA) with the acronym QPS (Qualified Presumption of Safety); they are also acid-tolerant bacteria [33,34]. From this point of view, they can be used for the enrichment of beverages based on acid whey.

The study hypothesis is that delivery systems loaded with a probiotic culture and a natural plant sweetener with prebiotic properties have potential application for the enrichment of fermented whey beverages and can impart beneficial properties to the final product.

2. Materials and Methods

2.1. Materials

Chitosan (5–20 mPa·s, 0.5% in 0.5% Acetic Acid at 20 °C), manufacturer Tokyo Chemical Industry Co., Ltd. (TCI), Tokyo, Japan.

Calcium chloride dihydrate, certified ACS, Thermo Fisher Scientific Inc., Waltham, MA, USA. Sigma-Aldrich (Merck, Darmstadt, Germany) supplied Sodium alginate powder (CAS Number: 9005-38-3, Viscosity 15–25 cps).

Bifidobacterium bifidum 791, which was proposed as a starter culture by Voblikova [35], was used as a probiotic microorganism, and the plant extract of *Stevia rebaudiana Bertoni* was used as an agent for co-encapsulation. These materials were provided by the laboratory “Biotechnology” of the M. Auezov South Kazakhstan University. To isolate bifidumbacteria, selective MRS (69964-500G, MRS Agar, suitable for microbiology, made in Switzerland, sigmaldrich.com) medium of a modified composition was used by adding cysteine (Sigma-Aldrich (Merck)), which is necessary for their growth, in anaerobic conditions. The release of the microencapsulated agent was studied in a phosphate-buffered solution (PBS). Standard PBS was prepared from sodium chloride, potassium chloride, potassium dihydrogen phosphate, and disodium hydrogen phosphate (Sigma-Aldrich (Merck)). All reagents were analytical grade, and used without additional purification.

2.2. Methods

2.2.1. Microcapsule Preparation

Microcapsules were prepared in a two-stage process via ion gelation and the complexation of polyelectrolytes at an ambient temperature, as described in [25]. *Bifidumbacterium* at a concentration of 1×10^8 CFU/g was added to 100 mL of sodium alginate solution (1.5%) and homogenized via gentle stirring with a magnetic stirrer for 60 min. Then, the suspension was dropped via a syringe pump (NE-1002X Programmable Microfluidics, New Era Pump Systems, Inc., Farmingdale, NY, USA) into 100 mL of 2% CaCl₂ solution as a cross-linking agent, under constant magnetic stirring, and the resulting microcapsules were washed with distilled water and filtered through a Buchner funnel (Coors™ Buchner funnel, Merck, Darmstadt, Germany).

In the second stage, the washed formulations were dispersed in 50 mL of chitosan solution (0.5% CS in 0.5% CH₃COOH (Sigma-Aldrich, Merck)) under constant stirring (magnetic stirrer). The chitosan in the formulations of the polymeric capsules provided the formation of polyelectrolyte complex shells of two polymers; this can stabilize the structure of the capsules, which have properties that maintain the integrity in an acidic environment simulating the stomach and dissolve in a medium simulating the pH of the intestines [36].

The microcapsules were prepared with different active agents: (CS/(ALG/(Ca + BB))); (CS/(ALG/(Ca + SE))); (CS/(ALG/(Ca + BB + SE))).

The release profile of the active agents from the microcapsules was studied in vitro by UV-Vis spectrophotometry ((UV-1900i dual-beam spectrophotometer with software (190–1100 nm), scanning speed up to 29,000 nm/m, manufacturer Shimadzu, Japan).

2.2.2. Determination of the Encapsulation Efficiency and Loading Capacity

The encapsulation efficiency (EE) was determined spectrophotometrically from the total concentration of active agents (c_{total}) and the content in the dried microcapsules (c_{load})

according to a method described by Vlahoviček-Kahlina et al. [24]. The encapsulation efficiency was calculated using the equations in [24]:

$$EE = (c_{load}/c_{total}) \times 100$$

$$c_{load} = c_{total} - c_f,$$

where c_f is the concentration of the active agent in the filtrate.

To determine the EE, the solution was stirred and left in the dark for 15 min, and the value on the spectrophotometer was read for samples with BB, SE, and BB + SE at $\lambda = 595$ nm.

The active agent contents (BB, BB + SE, and SE) in the microcapsule LC were determined by using a method described by Vlahoviček-Kahlina et al. [24]:

$$LC = w_{active\ agent}/w_c$$

where $w_{active\ agent}$ is the weight of loaded active agent and w_c is the weight of the microcapsules/beads.

2.2.3. Determination of the Degree of Swelling

The swelling process depends on the property of the dissolving agent, among other things. Therefore, to avoid the influence of the electrolytes in the buffer solutions, the degree of swelling (S_w) was determined for microcapsules dispersed in distilled water, as described by Kudasova et al. [25]. The microcapsules (10 mg) were transferred to test tubes, and they were allowed to swell at room temperature for three hours in 10 mL of distilled water to reach equilibrium. The weight of the wet swollen microcapsules was determined after removing the moisture from their surfaces with filter paper. S_w was calculated using a formula proposed by Vlahoviček-Kahlina et al. [24]:

$$S_w/\% = ((w_t - w_0)/w_0)$$

where w_t is the weight of swollen microcapsules and w_0 is the weight of the dry capsules.

All measurements were repeated three times, and the results are presented as the mean value with the corresponding standard deviation.

2.2.4. Fourier Transform Infrared Spectroscopy Analysis

Fourier transform infrared spectroscopy spectra were recorded with an infrared spectrometer, a Nicolet 5700 "Thermo Electron Corporation", Waltham, MA, USA, powered by OMNIC™ v9.x software, with the spectral field in the range of 500–4000 cm^{-1} .

2.2.5. Determination of Morphology

Analyses of the morphology, size, and shape of the wet and dry microcapsules were carried out with an optical microscope (Olympus Soft Imaging Solutions GmbH, version E_LCmicro_09Okt2009, Tokyo, Japan) immediately after their preparation and with a scanning electron microscope (SEM) (JEOL-SEM, JSM-6490 LV (Jeol Ltd., Tokyo, Japan), with INCA Energy 350 energy X-ray microanalysis (Oxford instruments, Oxford, UK) and HKL Basic (Oxford instruments, UK) and an SEM Quanta 3D 200i (Thermo Fisher Scientific, USA), after drying to a constant mass.

Scanning electron microscopy (Quanta 3D 200i) was carried out on all samples at an accelerating voltage of 15 keV and a working distance of ≈ 12 mm. All samples were secured with double-sided graphite 9 tape. All measurements were carried out in the high-vacuum mode at 10^{-3} Pa. The maximum magnification was $\times 5000$, and the minimum magnification was $\times 40$.

2.2.6. Release of Active Agents from the Microcapsules

The release profile of the active agents from the microcapsules was studied spectrophotometrically in vitro. Absorption spectra were measured at 595 nm to avoid damage to bacterial cells. All measurements were performed in phosphate-buffered solutions (pH 7.4).

In general, this study indicates that microencapsulation with an alginate-gelatinized starch coated with chitosan could successfully and significantly protect probiotic bacteria from adverse conditions simulating the human gastrointestinal environment.

2.2.7. Modeling the Behavior of Microcapsules with Active Agents in an Imitating Gastrointestinal Tract

The release kinetics of microcapsules in the imitating GIT have been modeled using a modified Higuchi model [37].

In this research, a linear model had been used based on the interpolation of selected data, which provides a precise approximation.

For a given time t , if $t_1 \leq t \leq t_2$, the release percentage $R_{(t)}$ is calculated as:

$$R_{(t)} = R_1 + \frac{R_2 - R_1}{t_2 - t_1} \times (t - t_1)$$

where t_1 and t_2 are the consecutive time points, R_1 is release percentage at t_1 , R_2 is the release percentage at t_2 , t is the studied time, and R_t is the calculated release percentage at time t .

The swelling behavior of the active agent loaded microcapsules have been modeled using an exponential function in dependence of time and pH of GIT [38]:

$$S_t = S_0 \times (1 + k \times (1 - e^{\alpha t}))$$

where $S_0 = 1$ —initial swelling factor, k is a constant related to the swelling capacity in dependence of GIT pH, and α is a rate constant (in the dependence of GIT pH), which shows how quickly the swelling occurs.

3. Results and Discussion

The studied systems were composed of sodium alginate (dry matter); calcium chloride; distilled water; Stevia powder; *Bifidumbacterium*; and the encapsulated agents (1) BB, (2) SE, and (3) BB + SE.

The physicochemical characteristics of microcapsules obtained according to the modified method [25] were studied.

3.1. Encapsulation Efficiency, Loading Capacity and Swelling Degree of Microcapsules

The loading efficiency and loading capacity were determined to obtain information on the yield and content of the active agents in the chitosan/alginate microcapsules. It is known that the entrapped amounts of active agents in chitosan/alginate microcapsules depend on the type and concentration of the gelling cation and active agents, as well as the preparation method [39].

The significant differences in the encapsulation efficiency (EE) and swelling degree (S_w) between the samples are shown in Tables 1 and 2. The difference in EE reflects the extent of electrostatic interactions and hydrogen bonds involved in the interactions of active agents with both calcium chloride and sodium alginate during the preparation. The most water-soluble active agent, BB + SE, exhibits the highest EE values, indicating a greater extent of molecular interactions in the solution. In addition to the molecular interactions, the encapsulation capacity also depends on the structure of the active agents.

Table 1. Encapsulation efficiency (EE) of the microcapsule formulation CS/(ALG/(Ca + active agent)).

Encapsulated Active Agent	EE ₁ , %	EE ₂ , %	EE ₃ , %	Average Value	Standard Deviation	Mean Square Deviation
BB	80.0	89.0	80.0	83.0	5.20	4.24
SE	89.6	88.09	89.0	89.2	0.38	0.31
BB + SE	90.0	92.0	92.0	91.3	1.15	0.94

Table 2. Swelling degree (S_w) of the microcapsule formulation CS/(ALG/(Ca + active agent)).

Encapsulated Active Agent	S_{w1} , %	S_{w2} , %	S_{w3} , %	Average Value	Standard Deviation	Mean Square Deviation
BB	76.9	80.0	80.0	79.0	1.78	1.45
SE	76.9	71.4	71.4	73.3	3.18	2.59
BB + SE	53.9	55.5	50.0	53.1	2.82	2.30

The encapsulation efficiency results—83.0% for *Bifidumbacterium* (BB), 89.2% for Stevia extract (SE), and an impressive 91.3% for their combination (BB + SE)—highlight the effectiveness of the encapsulation process. These results not only confirm the success of a well-optimized encapsulation method, as supported by previous studies [13,15,17], but they also underscore the innovative potential of co-encapsulation in enhancing the functionality of bioactive compounds.

The highest encapsulation efficiency observed with BB + SE co-encapsulation suggests a synergistic effect, likely resulting from complementary interactions between the probiotic and the plant extract during the encapsulation process. These interactions appear to enhance both retention and stability of the active agents within the microcapsules, as noted by Xu et al. [40]. Additionally, Stevia extract seems to increase the matrix's affinity for bacterial cells, further improving encapsulation efficiency, as highlighted by Yao et al. [15]. This superior encapsulation efficiency is particularly beneficial for functional food applications, where maintaining the stability and controlled release of probiotics is crucial for delivering sustained health benefits [41].

The enhanced encapsulation efficiency is further corroborated by the lower swelling degree observed in the BB + SE microcapsules (53.1%), compared to microcapsules containing only BB (79.0%) or SE (73.3%). This reduced swelling can be attributed to stronger intermolecular interactions and enhanced cross-linking within the microcapsule matrix, as co-encapsulation of multiple active agents often leads to a more compact structure [14]. The lower swelling degree is advantageous for applications requiring controlled release and prolonged stability, as it typically correlates with slower release rates and better retention of encapsulated materials [12,41].

Moreover, the co-encapsulation of BB and SE results in the formation of larger microcapsules with a lower moisture content (approximately 55%), compared to the smaller, more hydrated microcapsules containing only BB (up to 77% moisture). This difference suggests that co-encapsulation promotes a more compact and less hydrated microcapsule structure, likely due to the enhanced interactions between the encapsulated components and the matrix. The larger size and reduced moisture content of the BB + SE microcapsules may contribute to improved stability and controlled release, further supporting their potential effectiveness in delivering active agents in functional food applications.

3.2. FTIR Characterization of Microcapsules Encapsulating BB, SE, and Their Combination BB + SE

Fourier transform infrared spectroscopy (FTIR) provides information for the identification of chemical bonds according to the infrared absorption spectrum. The spectra reveal the profile of a sample containing various components. The spectra of the BB, SE, and their mixtures with core components are presented and discussed in Figure 1.

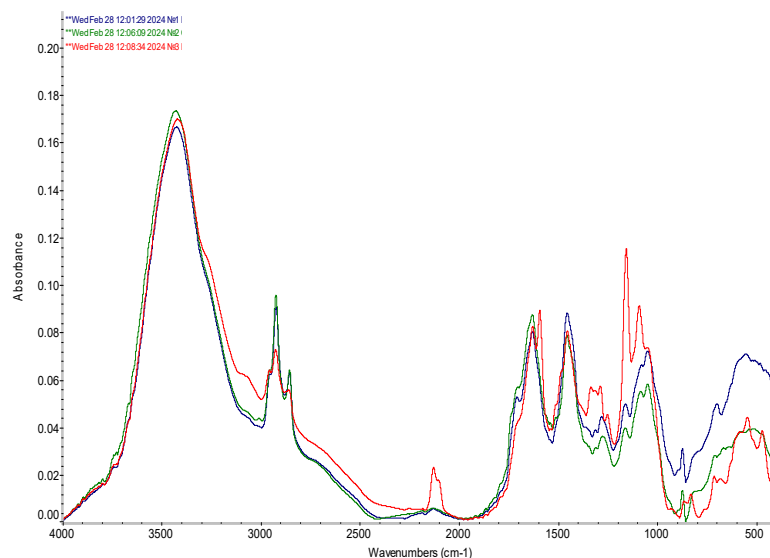


Figure 1. FTIR spectra of microcapsules loaded with *Bifidumbacterium*, Stevia extract, and mixture of *Bifidumbacterium* with Stevia extract. N°1 *Bifidumbacterium bifidum* (BB); N°2 Stevia extract (SE); N°3 BB + SE.

The FTIR spectra of the microcapsules containing BB exhibit a notable peak near 3413.9 cm^{-1} , corresponding to primary NH stretching, two peaks at 2978.6 and 2900.8 cm^{-1} , which were assigned to the CH_3 asymmetric stretching vibration [42,43]. The peak near 1650 cm^{-1} , associated with the CO stretching of primary amides present in the proteins of the bacterial cell membrane. The presence of nitrile groups in the spectra is evidenced by an absorption peak at 2127 cm^{-1} , within the expected triple-bond region of $2300\text{--}2000\text{ cm}^{-1}$. All of these peaks indicate significant interactions between the alginate, chitosan, and the encapsulated BB, confirming the formation of stable bonds within the microcapsule matrix. These data are consistent with findings reported by authors [44], and the amide I and II peaks are typical for proteins in microbial cells, as described in the literature [45,46].

Further analysis of the spectra shows important vibrational modes around 1460 and 1380 cm^{-1} , attributed to C-H deformation. These modes are important for confirming the structural integrity of the encapsulation matrix. The vibrational modes at 1084.5 and 1046.5 cm^{-1} , corresponding to OH deformation vibrations, are characteristic of primary (1050 cm^{-1}) and secondary alcohols (1100 cm^{-1}). These modes are closely associated with polysaccharide vibrations, aligning with previous studies on carbohydrate spectroscopy [42,47,48].

The FTIR spectrum of the encapsulated SE reveals a distinct peak at 1644.2 cm^{-1} , corresponding to the CO stretching of the carboxylic group, which results from the hydrolysis of the alginate within the encapsulation matrix, indicating interactions between SE and the alginate. Additionally, the bands observed at 1452.6 and 1402.4 cm^{-1} are attributed to CH deformation modes, further confirming the structural integrity of the encapsulated material.

The wavelength at 2120 cm^{-1} indicates the presence of isothiocyanate groups, which are known to be associated with substances found in Stevia. This observation is particularly significant as it highlights the successful encapsulation and preservation of bioactive compounds within the SE, potentially enhancing the functional properties of the encapsulated product.

The displacement of bands at 3402.7 at BB + SE microcapsules suggests the presence of amide groups, originating from the proteins in the cell membrane of BB, and effect of SE, further confirming the effective encapsulation of the active agents within the matrix [49]. The broad peaks in the range of $3000\text{--}3600\text{ cm}^{-1}$, observed in these spectra, are indicative of the combined effects of O-H and N-H stretching, which overlap with polysaccharide backbone vibrations, which is consistent with the data reported by Moreno et al. [44] and other studies [50].

The appearance of three peaks at range of 2898.5–2929.8 cm^{-1} testified about interactions between BB, SE and components of encapsulating materials. The peak at 2977 cm^{-1} corresponds to the CH_3 asymmetric stretching, and is supported by a CH_2 absorption band around 2929.8 cm^{-1} , the peak at 2898.5 cm^{-1} , associated with symmetric CH_3 vibration, confirms the presence of lipid components within the membrane of the encapsulated agents, as mentioned in studies [44,51]. These lipid-associated peaks indicate the retention of critical membrane structures, which are essential for maintaining the viability and functionality of the encapsulated active agents.

The peak at 1649.8 cm^{-1} , corresponding to the CO stretching of primary amide groups, confirms the intermolecular interactions between the active agents and the encapsulation matrix composed of alginate and chitosan. This finding is in line with previous reports [42,45], where amide I and amide II bands are recognized as typical for all proteins, confirming the presence of proteinaceous components within both the BB and BB + SE.

The four small peaks at 1452.2 cm^{-1} , 1383.9 cm^{-1} , 1329.1 cm^{-1} and 1274.0 cm^{-1} suggest complex interactions between the encapsulated agents and the biopolymer matrix, which may enhance the structural integrity and stability of the microcapsules.

The peak at 1452.2 cm^{-1} corresponds to the CH_2 scissor vibration, which overlaps the CH_3 asymmetric deformation, while the peak at 1383.9 cm^{-1} corresponds to the symmetric CH_3 vibration.

The peak at 1274.0 cm^{-1} corresponds to secondary amide III vibrations, which are typically found near 1270 cm^{-1} , as reported in the literature [52]. This peak, along with others in the region of 1200–950 cm^{-1} , corresponds to the various vibrational modes of polysaccharides and polysaccharide-containing biomolecular complexes. The consistent appearance of peaks at 1280.3 cm^{-1} for BB, 1277 cm^{-1} for SE, and 1287.1 cm^{-1} for BB + SE indicates a strong correlation between these bands and the interactions within the encapsulation matrix.

The peaks at 880.0 and 670.9 correspond to the characteristic peaks of alginate and the NH deformational vibrations of chitosan, respectively. These peaks can be found in the cases of BB, SE, and BB + SE microcapsules, confirming the successful formation of an alginate-chitosan (Alg/CS) shell, resulting from interactions between oppositely charged carbonyl groups of alginate and the amino groups of chitosan. This interaction is essential for the structural integrity of the microcapsules, where the formation of polyelectrolyte complexes between alginate and chitosan was observed.

When comparing the spectra of the microcapsules containing active agents (BB, SE, and BB + SE) with those of hollow microcapsules, as described by the authors of [24], it is evident that the active agent-loaded microcapsules exhibit more intense bands. This suggests stronger intermolecular interactions and possibly a higher degree of cross-linking within the matrix. Moreover, the polysaccharide mixtures described by the authors of [50] show some spectral differences compared to the active agent-loaded microcapsules, highlighting the impact of the encapsulated agents on the overall structure and vibrational properties of the microcapsules.

The FTIR analysis of the BB + SE microcapsules reveals significant shifts in peak positions compared to the spectra of SE and BB when encapsulated separately, as well as to the spectra of hollow microcapsules.

In all three cases, distinct vibration peaks were observed, which reflect the presence of strong intermolecular interactions between the microcapsule components. These interactions contribute to the stability and functionality of the encapsulation system.

3.3. Morphological Studies

The micrographs show the morphology, size, and shape of the wet microcapsules immediately after their preparation and after drying. All wet microcapsules were almost spherical, and their surface was smooth and dense. The smooth surface was a consequence of the chitosan binding to sodium alginate chains [24,25]. Microspheres and coated microspheres are usually spherical with different surface morphologies.

Figures 2–4 display scanning electron microscope (SEM) images of the dehydrated microcapsules. The dimensions of the microcapsules observed through a scanning electron microscope (SEM) are consistent with those observed through an optical microscope (OM). The image of the microcapsules containing chitosan/alginate formulations loaded with active agents shows diameters in a range between 650 μm and 1.1 mm.

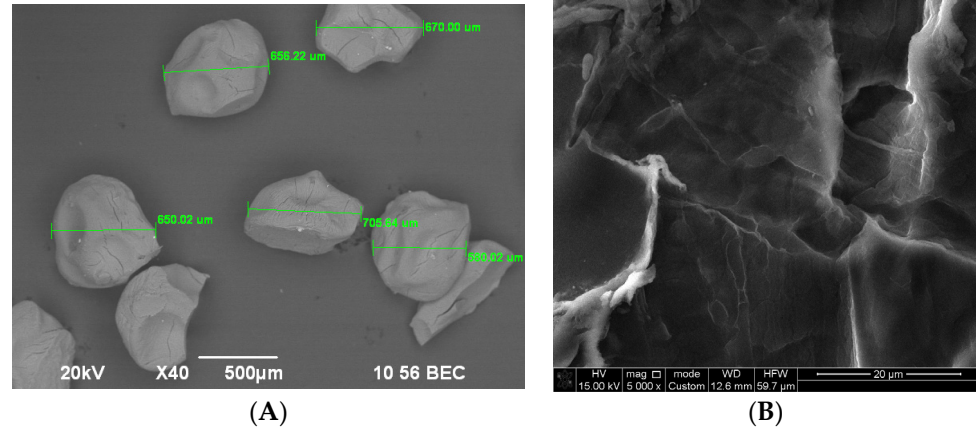


Figure 2. Image of Stevia extract-loaded microcapsules: (A)—microcapsule diameters (at a magnification of 40); (B)—microcapsule porous surface (at a magnification of 5000).

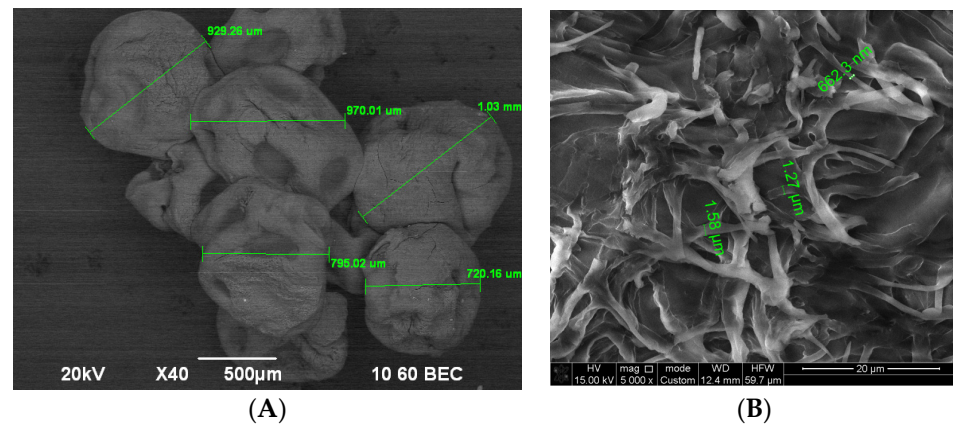


Figure 3. SEM microphotograph of dry microcapsules prepared with BB: (A)—microcapsule diameters (at a magnification of 40); (B)—microcapsule porous surface (at a magnification of 5000).

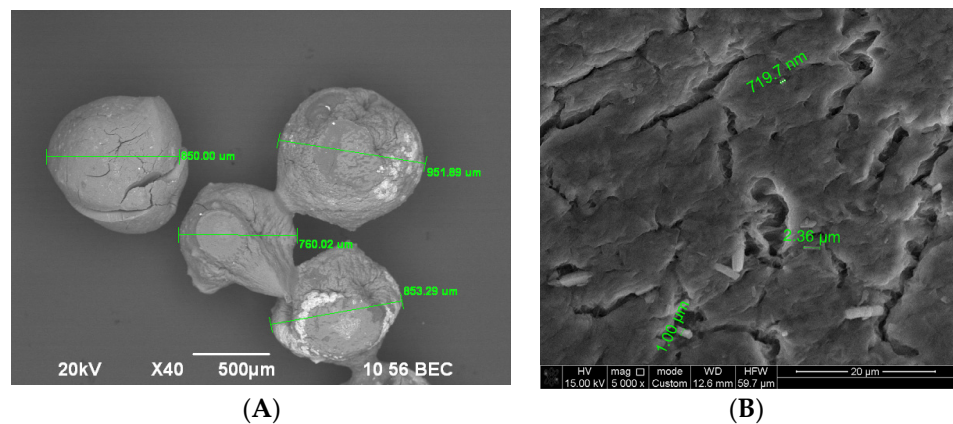


Figure 4. SEM microphotograph of dry microcapsules prepared with BB + SE: (A)—microcapsule diameters (at a magnification of 40); (B)—microcapsule porous surface (at a magnification of 5000).

Figure 2 shows images of the microcapsules taken with a scanning electron microscope (SEM) after being dried for about a week at room temperature until they reached a

constant mass. It is evident that they underwent a loss of their spherical morphology and significantly reduced in size compared to the wet capsules.

From Figure 2, it can be seen that the diameter of the SE-loaded microcapsules ranges from 650 to 706 μm . Figure 3 shows the BB-loaded microcapsules with different diameters.

Figure 4B shows the porous surface structure of the BB + SE-loaded dried microcapsules, with diameters of depressions on the surface varying between 719 nm and 2.36 μm . The surfaces of the microcapsules were spherical in shape and were stable when squeezed, which is consistent with data described in [24].

The color of the microcapsules (BB + SE) was yellowish, and, after drying, they became green-yellow due to the entrapped Stevia extract. In contrast, the wet microcapsules produced with BB were whitish in color, and, after drying, they developed a light yellow tone. The surfaces of the dry microcapsules were not smooth, and wrinkles could be observed. This can be explained by the fact that the produced microcapsules contained approximately 55–77% water. After the evaporation of liquid and moisture, the diameters of all prepared microcapsules decreased by half; this is associated with the relaxation–deformation process of the biopolymers, i.e., by the partial collapse of the polymer network during dehydration [53].

Produced by this method, porous dry microcapsules are suitable for living microorganisms and contribute to protection, stability and prolongation of action during use.

3.4. Release of Active Agents from Microcapsules

The release kinetics and mechanism of the active agent primarily depend on the characteristics of the core material and the active agent. For a hydrophilic biopolymer matrix, the active components are uniformly distributed/dissolved in the gel matrix, and the release is governed by diffusion, swelling, and matrix erosion as described in [24].

Figure 5 shows the release kinetics of active agents (BB, SE, and BB + SE) from microcapsules as a function of time exhibited a continuous and gradual release pattern. Within the initial period of two hours, approximately 38% of BB and SE were released, which increased to approximately 55–58% after four hours. This can be assumed a steady diffusion of the active agents through the gel matrix. For BB + SE, as a combination of active agents, the release showed faster kinetics. Within two hours, around 60% of the active agents were released, and this value further increased to 70% after four hours. This accelerated release may be explained by a synergistic effect between BB and SE, which could enhance the permeability of the encapsulation matrix or alter the internal microenvironment, facilitating a quicker diffusion of the active agents. After 24 h, BB + SE combination were released almost completely, indicating that the microcapsules were effective in providing a required release, ensuring that a significant amount of the active agents are available at the desired period.

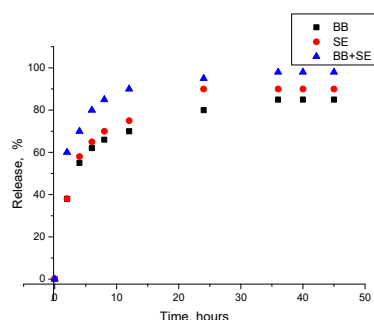


Figure 5. Release kinetics of active agents over time: BB, SE, and BB + SE.

From the literature, it is known that food generally stays in the stomach for between 40 min and 2 h. It then spends around five hours in the small intestine, before passing through the colon, which can take between 10 and 59 h [54]. Thus, release over 24 h is enough for probiotics' survival.

Thus, research findings of release kinetics show that microcapsules produced by loading of a combination of BB + SE can have controlled release.

3.5. Behavior of Active Agents Loaded Microcapsules in an Imitating Gastrointestinal Tract

The next release percentage $R_{(t)}$ using piecewise linear function have been calculated: $R_{BB(t)} = R_{SE(t)} = R_{(BB + SE)(t)}$: for $2 \leq t \leq 4$ and for $4 \leq t \leq 24$.

Information about swelling behavior of the active agent loaded microcapsules have been modeled using an exponential function in dependence of time and pH of GIT as presented in Table 3.

Table 3. Parameters for swelling behavior of microcapsules in different sections of the GIT.

Section of GIT	pH	k	α
Stomach	1–3	0.5 ± 0.1	0.15 ± 0.0361
Small intestine	6–7	0.3 ± 0.1	0.1 ± 0.0361
Colon intestine	6–7.5	0.4 ± 0.1	0.08 ± 0.0361

Modeling of swelling behavior at different GIT sections has shown that in the stomach section the $\alpha = 0.15$ testified about rapid swelling because of high acidity. In the small intestine, this value is equal to 0.10, which confirms moderate swelling, and $\alpha = 0.08$ testified about slow release.

Design of release kinetics and swelling behavior show that the developed microcapsules are suitable for the controlled release of BB, SE and BB + SE in a simulated GI tract. Initially, there is a rapid release in the stomach, which is associated with high acidity. This is followed by a slow release in the small and colon intestines, which provides optimal conditions for probiotic survival and activity. Thus, the design results show that the developed microcapsules are effective in application.

4. Conclusions

The study results successfully demonstrated the potential of encapsulating *Bifidumbacteria* (BB) and stevia extract (SE) into alginate-chitosan microcapsules for use in fermented beverage fortification. FTIR analysis confirmed significant interactions between the encapsulated agents and the biopolymer matrix, indicating the formation of a stable and efficient encapsulation system. The high encapsulation efficiencies observed (83.0% for BB, 89.2% for SE, and 91.3% for BB + SE) reflect the reliability of the system for protection and enhancing the survivability of active agents in the aggressive environment. Particularly for the co-encapsulation of BB and SE, the synergistic effect likely enhanced the stability and retention of the active agents within microcapsules.

The swelling degree of the capsules loaded with BB was 79%, that of the capsules loaded with SE was 73%, and that of the capsules loaded with BB + SE was 53%. This lower swelling and moisture content indicate a more compact and stable structure. This compact structure was further supported by the observed wrinkled porous surface morphology, resulting from the partial collapse of the polymer network during the drying process.

The morphology of the dry capsules showed that there were cracks on the surface, with diameters between 719.7 nm and 2.36 μm . In addition, there were recesses, with widths between 81 and 127 μm and lengths from 162 to 384 μm .

The release kinetics of the microcapsules demonstrated a controlled and sustained release over 24 h, aligning with the transit time of food through the gastrointestinal tract. The faster initial release observed in the BB + SE microcapsules suggests potential synergistic interactions that could be advantageous in applications requiring a release at desired time.

Modeling of release kinetics and swelling behavior of microcapsules in the imitating GIT show that the developed microcapsules are suitable for the protection of active agents at application in the enrichment of fermented beverage.

The encapsulation of probiotic bacteria and plant extracts lays the groundwork for innovative applications in the fortification of fermented beverages. These beverages will

be developed using acid whey, a byproduct of the dairy industry that is notably rich in essential micro- and macro-elements. By repurposing acid whey, this research not only contributes to waste reduction but also enhances the nutritional value of the resulting fermented products.

The novelty of this investigated encapsulation system is the increased stability, bioavailability, and functionality of the active agents, which provides a foundation for the development of functional fermented beverages enriched with probiotics and plant extracts, offering health benefits for consumers.

Author Contributions: Conceptualization, B.M. and E.T.; methodology, E.T. and B.M.; software, A.I. and A.S.; validation, G.M., B.M. and S.A.; formal analysis, B.M., E.T.; investigation, E.T., D.O., G.M. and B.M.; resources, B.M. and G.M.; data curation, B.M., E.T., G.M.; writing—original draft preparation, E.T. and B.M.; writing—review and editing, B.M., R.M., G.M. and A.I.; visualization, E.T., B.M. and R.M.; supervision, B.M.; project administration, G.M. and B.M.; funding acquisition, G.M. All authors have read and agreed to the published version of the manuscript.

Funding: This research is funded by the Science Committee of the Ministry of Science and Higher Education of the Republic of Kazakhstan (Grant No. AP19679879).

Data Availability Statement: The original contributions presented in the study are included in the article, further inquiries can be directed to the corresponding author/s.

Conflicts of Interest: The authors declare no conflicts of interest.

References

1. Solieri, L.; Valentini, M.; Cattivelli, A.; Sola, L.; Helal, A.; Martini, S.; Tagliazucchi, D. Fermentation of whey protein concentrate by *Streptococcus thermophilus* strains releases peptides with biological activities. *Process. Biochem.* **2022**, *121*, 590–600. [[CrossRef](#)]
2. Jitpakdee, J.; Kantachote, D.; Kanzaki, H.; Nitoda, T. Potential of lactic acid bacteria to produce functional fermented whey beverage with putative health promoting attributes. *LWT* **2022**, *160*, 113269. [[CrossRef](#)]
3. Skryplonek, K.; Dmytrów, I.; Mituniewicz-Małek, A. Probiotic fermented beverages based on acid whey. *J. Dairy Sci.* **2019**, *102*, 7773–7780. [[CrossRef](#)] [[PubMed](#)]
4. Shi, X.; Wu, D.; Xu, Y.; Yu, X. Engineering the optimum pH of β -galactosidase from *Aspergillus oryzae* for efficient hydrolysis of lactose. *J. Dairy Sci.* **2022**, *105*, 4772–4782. [[CrossRef](#)]
5. Wherry, B.; Barbano, D.M.; Drake, M.A. Use of acid whey protein concentrate as an ingredient in nonfat cup set-style yogurt. *J. Dairy Sci.* **2019**, *102*, 8768–8784. [[CrossRef](#)] [[PubMed](#)]
6. Molero, M.S.; Briñez, W.J. Probiotics Consumption Increment through the Use of Whey-Based Fermented Beverages. In *Probiotics—Current Knowledge and Future Prospects*; InTech: Houston, TX, USA, 2018. [[CrossRef](#)]
7. Food and Agriculture Organization of the United Nations; World Health Organization. *Guidelines for the Evaluation of Probiotics in Food*; Food and Agriculture Organization of the United Nations: Rome, Italy; World Health Organization: Geneva, Switzerland, 2002.
8. Saad, S.M.I. Probiotics and prebiotics: The state of the art. *Braz. J. Pharm. Sci.* **2006**, *42*, 1–16.
9. Mgomi, F.C.; Yuan, L.; Farooq, R.; Lu, C.-L.; Yang, Z.-Q. Survivability and characterization of the biofilm-like probiotic *Pediococcus pentosaceus* encapsulated in calcium alginate gel beads. *Food Hydrocoll.* **2024**, *156*, 110253. [[CrossRef](#)]
10. Shori, A.B. Microencapsulation improved probiotics survival during gastric transit. *J. Biosci.* **2017**, *24*, 1–5. [[CrossRef](#)]
11. da Silva, M.N.; Tagliapietra, B.L.; Flores, V.D.A.; Richards, N.S.P.d.S. In vitro test to evaluate survival in the gastrointestinal tract of commercial probiotics. *Curr. Res. Food Sci.* **2021**, *4*, 320–325. [[CrossRef](#)]
12. Champagne, C.P.; Gomes da Cruz, A.; Daga, M. Strategies to improve the functionality of probiotics in supplements and foods. *Curr. Opin. Food Sci.* **2018**, *22*, 160–166. [[CrossRef](#)]
13. Krunić, T.Ž.; Rakin, M.B. Enriching alginate matrix used for probiotic encapsulation with whey protein concentrate or its trypsin-derived hydrolysate: Impact on antioxidant capacity and stability of fermented whey-based beverages. *Food Chem.* **2022**, *370*, 130931. [[CrossRef](#)] [[PubMed](#)]
14. Zanjani, M.; Tarzia, B.; Sharifana, A.; Mohammadi, N. Microencapsulation of Probiotics by Calcium Alginate-gelatinized Starch with Chitosan Coating and Evaluation of Survival in Simulated Human Gastro-intestinal Condition. *Iran J. Pharm. Res. (IJPR)* **2014**, *13*, 843–852.
15. Yao, M.; Xie, J.; Du, H.; McClements, D.J.; Xiao, H.; Li, L. Progress in microencapsulation of probiotics: A review. *Compr. Rev. Food Sci. Food Saf.* **2020**, *19*, 857–874. [[CrossRef](#)] [[PubMed](#)]
16. Alemzadeh, E.; Oryan, A. Application of encapsulated probiotics in health care. *J. Exp. Path.* **2020**, *1*, 16–21.
17. Ding, W.K.; Shah, N.P. Effect of Various Encapsulating Materials on the Stability of Probiotic Bacteria. *J. Food Sci.* **2009**, *74*, M100–M107. [[CrossRef](#)]

18. Gaonkar, A.; Vasisht, N.; Khare, A.; Sobel, R. *Microencapsulation in the Food Industry*, 1st ed.; A Practical Implementation Guide; Academic Press: Cambridge, MA, USA, 2014.
19. Ozdal, T.; Yolci-Omeroglu, P.; Tamer, E.C. 6-Role of Encapsulation in Functional Beverages. In *Biotechnological Progress and Beverage Consumption*; Grumezescu, A.M., Holban, A.M., Eds.; Academic Press: Cambridge, MA, USA, 2020; pp. 195–232. [[CrossRef](#)]
20. Nezamdoost-Sani, N.; Khaledabad, M.A.; Amiri, S.; Mousavi Khaneghah, A. Alginate and derivatives hydrogels in encapsulation of probiotic bacteria: An updated review. *Food Biosci.* **2023**, *52*, 102433. [[CrossRef](#)]
21. Amiri, S.; Abotalebi Kohneshahri, S.R.; Nabizadeh, F. The effect of unit operation and adjunct probiotic culture on physicochemical, biochemical, and textural properties of Dutch Edam cheese. *LWT* **2022**, *155*, 112859. [[CrossRef](#)]
22. Thambiliyagodage, C.; Jayanetti, M.; Mendis, A.; Ekanayake, G.; Liyanaarachchi, H.; Vigneswaran, S. Recent Advances in Chitosan-Based Applications—A Review. *Materials* **2023**, *16*, 2073. [[CrossRef](#)]
23. Xie, A.; Zhao, S.; Liu, Z.; Yue, X.; Shao, J.; Li, M.; Li, Z. Polysaccharides, proteins, and their complex as microencapsulation carriers for delivery of probiotics: A review on carrier types and encapsulation techniques. *Int. J. Biol. Macromol.* **2023**, *242*, 124784. [[CrossRef](#)]
24. Vlahoviček-Kahlina, K.; Jurić, S.; Marijan, M.; Mutaliyeva, B.; Khalus, S.V.; Prosyanič, A.V.; Vinceković, M. Synthesis, Characterization, and Encapsulation of Novel Plant Growth Regulators (PGRs) in Biopolymer Matrices. *Int. J. Mol. Sci.* **2021**, *22*, 1847. [[CrossRef](#)]
25. Kudasova, D.; Mutaliyeva, B.; Vlahoviček-Kahlina, K.; Jurić, S.; Marijan, M.; Khalus, S.V.; Prosyanič, A.V.; Šegota, S.; Španić, N.; Vinceković, M. Encapsulation of Synthesized Plant Growth Regulator Based on Copper(II) Complex in Chitosan/Alginate Microcapsules. *Int. J. Mol. Sci.* **2021**, *22*, 2663. [[CrossRef](#)]
26. Ta, L.P.; Bujna, E.; Antal, O.; Ladányi, M.; Juhász, R.; Szécsi, A.; Kun, S.; Sudheer, S.; Gupta, V.K.; Nguyen, Q.D. Effects of various polysaccharides (alginate, carrageenan, gums, chitosan) and their combination with prebiotic saccharides (resistant starch, lactosucrose, lactulose) on the encapsulation of probiotic bacteria *Lactobacillus casei* 01 strain. *Int. J. Biol. Macromol.* **2021**, *183*, 1136–1144. [[CrossRef](#)] [[PubMed](#)]
27. Peredo, A.; Beristain, C.; Pascual, L.; Azuara, E.; Jimenez, M. The effect of prebiotics on the viability of encapsulated probiotic bacteria. *LWT* **2016**, *73*, 191–196. [[CrossRef](#)]
28. Ismail, S.A.; Hassan, A.A.; Nour, S.A.; El-Sayed, H.S. The production of stirred yogurt fortified with prebiotic xylooligosaccharide, probiotic and synbiotic microcapsules. *Biocatal. Agric. Biotechnol.* **2023**, *50*, 102729. [[CrossRef](#)]
29. Zhou, Z.; Sarwar, A.; Xue, R.; Hu, G.; Wu, J.; Aziz, T.; Alasmari, A.F.; Yang, Z.; Yang, Z. Metabolomics analysis of potential functional metabolites in synbiotic ice cream made with probiotic *Saccharomyces cerevisiae* var. *boulardii* CNCM I-745 and prebiotic inulin. *Food Chem.* **2024**, *454*, 139839. [[CrossRef](#)] [[PubMed](#)]
30. Prakash, K.S.; Bashir, K.; Mishra, V. Development of symbiotic litchi juice drink and its physicochemical, viability and sensory analysis. *J. Food Process. Technol.* **2017**, *8*, 1–6. [[CrossRef](#)]
31. Kurek, J.M.; Krejpcio, Z. The functional and health-promoting properties of Stevia rebaudiana Bertoni and its glycosides with special focus on the antidiabetic potential—A review. *J. Funct. Foods* **2019**, *61*, 103465. [[CrossRef](#)]
32. Jungersen, M.; Wind, A.; Johansen, E.; Christensen, J.E.; Stuer-Lauridsen, B.; Eskesen, D. The Science behind the Pro-biotic Strain Bifidobacterium Animalis Subsp. Lactis BB-12[®]. *Microorganisms* **2014**, *2*, 92–110. [[CrossRef](#)]
33. Matera, M. *Bifidobacteria, Lactobacilli... When, How and Why to Use Them*; Global Pediatrics: New York, NY, USA, 2024; Volume 8, p. 100139. [[CrossRef](#)]
34. Pyle, S. 2.23-Human Gut Microbiota and the Influence of Probiotics, Prebiotics, and Micronutrients. *Compr. Gut Microbiota* **2022**, *2*, 271–288. [[CrossRef](#)]
35. Voblikova, T. Viability of the culture of Bifidobacterium bifidum immobilized by microencapsulation in dairy drink and the simulated gastrointestinal liquids. *Vestnik MGTU* **2019**, *22*, 305–313. [[CrossRef](#)]
36. Hamman, J. Chitosan Based Polyelectrolyte Complexes as Potential Carrier Materials in Drug Delivery Systems. *Mar Drugs* **2010**, *8*, 1305–1322. [[CrossRef](#)] [[PubMed](#)]
37. Higuchi, T. Mechanism of sustained-action medication. Theoretical analysis of rate of release of solid drugs dispersed in solid matrices. *J. Pharm. Sci.* **1963**, *52*, 1145–1149. [[CrossRef](#)]
38. Fu, J.; Cai, Y.; Le, Q.; Su, Z. Controlled release behavior of a pH-sensitive hydrogel microsphere based on modified alginate. *Int. J. Biol. Macromol.* **2018**, *112*, 218–225. [[CrossRef](#)]
39. Aguilera, D.A.; Di Sante, L.S.; Pettignano, A.; Riccioli, R.; Roeske, J.; Albergati, L.; Corti, V.; Fochi, M.; Bernardi, L.; Quignard, F.; et al. Adsorption of a Chiral Amine on Alginate Gel Beads and Evaluation of its Efficiency as Heterogeneous Enantioselective Catalyst. *Eur. J. Org. Chem.* **2019**, *2019*, 3842–3849. [[CrossRef](#)]
40. Xu, C.; Ban, Q.; Wang, W.; Hou, J.; Jiang, Z. Novel nano-encapsulated probiotic agents: Encapsulate materials, delivery, and encapsulation systems. *J. Control. Release* **2022**, *349*, 184–205. [[CrossRef](#)]
41. Burgain, J.; Corgneau, M.; Scher, J.; Gaiani, C. *Chapter 20—Encapsulation of Probiotics in Milk Protein Microcapsules*; Academic Press: Cambridge, MA, USA, 2015. [[CrossRef](#)]
42. Kamnev, A.A.; Dyatlova, Y.A.; Kenzhegulov, O.A.; Vladimirova, A.A.; Mamchenkova, P.V.; Tugarova, A.V. Fourier Transform Infrared (FTIR) Spectroscopic Analyses of Microbiological Samples and Biogenic Selenium Nanoparticles of Microbial Origin: Sample Preparation Effects. *Molecules* **2021**, *26*, 1146. [[CrossRef](#)]

43. Kamnev, A.A.; Dyatlova, Y.A.; Kenzhegulov, O.A.; Fedonenko, Y.P.; Evstigneeva, S.S.; Tugarova, A.V. Fourier Transform Infrared (FTIR) Spectroscopic Study of Biofilms Formed by the Rhizobacterium *Azospirillum baldaniorum* Sp245: Aspects of Methodology and Matrix Composition. *Molecules* **2023**, *28*, 1949. [[CrossRef](#)]
44. Moreno, J.S.; Dima, P.; Chronakis, I.S.; Mendes, A.C. Electrospayed Ethyl Cellulose Core-Shell Microcapsules for the Encapsulation of Probiotics. *Pharmaceutics* **2022**, *14*, 7. [[CrossRef](#)]
45. Naumann, D. Infrared Spectroscopy in Microbiology. In *Encyclopedia of Analytical Chemistry*; Wiley: Hoboken, NJ, USA, 2006. [[CrossRef](#)]
46. Barth, A. Infrared spectroscopy of proteins. *Biochim. Biophys. Acta Bioenerg.* **2007**, *1767*, 1073–1101. [[CrossRef](#)]
47. Naumann, D.; Helm, D.; Labischinski, H. Microbiological characterizations by FT-IR spectroscopy. *Nature* **1991**, *351*, 81–82. [[CrossRef](#)]
48. Wiercigroch, E.; Szafraniec, E.; Czamara, K.; Pacia, M.Z.; Majzner, K.; Kochan, K.; Kaczor, A.; Baranska, M.; Malek, K. Raman and infrared spectroscopy of carbohydrates: A review. *Spectrochim. Acta Part A Mol. Biomol. Spectrosc.* **2017**, *185*, 317–335. [[CrossRef](#)]
49. Gordon, S.H.; Harry-O'kuru, R.E.; Mohamed, A.A. Elimination of interference from water in KBr disk FT-IR spectra of solid biomaterials by chemometrics solved with kinetic modeling. *Talanta* **2017**, *174*, 587–598. [[CrossRef](#)] [[PubMed](#)]
50. Baysal, K.; Aroguz, A.; Adiguzel, Z.; Baysal, B. Chitosan/Alginate Crosslinked Hydrogels: Preparation, Characterization and Application for Cell Growth Purposes. *Int. J. Biol. Macromol.* **2013**, *59*, 342–348. [[CrossRef](#)] [[PubMed](#)]
51. Vodnar, D.; Adriana, P.; Francisc, D.; Socaciu, C. HPLC Characterization of Lactic Acid Formation and FTIR Fingerprint of Probiotic Bacteria during Fermentation Processes. *Not. Bot. Horti Agrobot. Cluj Napoca* **2010**, *38*, 109–113.
52. Yin, M.; Chen, L.; Chen, M.; Yuan, Y.; Liu, F.; Zhong, F. Encapsulation of *Lactobacillus rhamnosus* GG in double emulsions: Role of prebiotics in improving probiotics survival during spray drying and storage. *Food Hydrocoll.* **2024**, *151*, 109792. [[CrossRef](#)]
53. Jurić, S.; Šegota, S.; Vinceković, M. Influence of surface morphology and structure of alginate microparticles on the bioactive agents release behavior. *Carbohydr. Polym.* **2019**, *218*, 234–242. [[CrossRef](#)]
54. Mackie, A.; Mulet-Cabero, A.-I.; Torcello-Gómez, A. Simulating human digestion: Developing our knowledge to create healthier and more sustainable foods. *Food Funct.* **2020**, *11*, 9397–9431. [[CrossRef](#)]

Disclaimer/Publisher's Note: The statements, opinions and data contained in all publications are solely those of the individual author(s) and contributor(s) and not of MDPI and/or the editor(s). MDPI and/or the editor(s) disclaim responsibility for any injury to people or property resulting from any ideas, methods, instructions or products referred to in the content.